

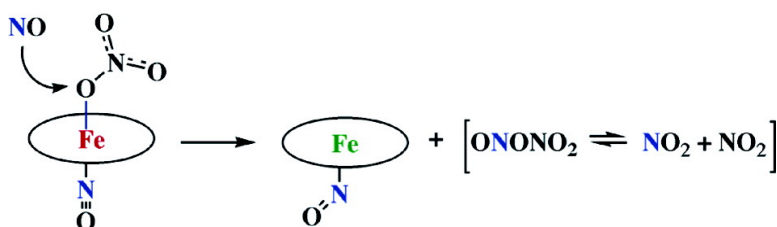
Article

Reactions of Nitrogen Oxides with Heme Models. Spectral and Kinetic Study of Nitric Oxide Reactions with Solid and Solute Fe(TPP)(NO)

Tigran S. Kurtikyan, Gurgen M. Gulyan, Garik G. Martirosyan, Mark D. Lim, and Peter C. Ford

J. Am. Chem. Soc., **2005**, 127 (17), 6216-6224 • DOI: 10.1021/ja042237r • Publication Date (Web): 09 April 2005

Downloaded from <http://pubs.acs.org> on March 25, 2009



More About This Article

Additional resources and features associated with this article are available within the HTML version:

- Supporting Information
- Links to the 4 articles that cite this article, as of the time of this article download
- Access to high resolution figures
- Links to articles and content related to this article
- Copyright permission to reproduce figures and/or text from this article

[View the Full Text HTML](#)

Reactions of Nitrogen Oxides with Heme Models. Spectral and Kinetic Study of Nitric Oxide Reactions with Solid and Solute $\text{Fe}^{\text{III}}(\text{TPP})(\text{NO}_3)$

Tigran S. Kurtikyan,^{*,†,‡} Gurgen M. Gulyan,[†] Garik G. Martirosyan,[†]
Mark D. Lim,[§] and Peter C. Ford^{*,§}

Contribution from the Research Institute of Applied Chemistry (ARIAC), 375005, Yerevan, Armenia, Molecule Structure Research Centre (MSRC) NAS, 375014, Yerevan, Armenia, and Department of Chemistry and Biochemistry, University of California, Santa Barbara, California 93106

Received December 24, 2004; E-mail: tkurt@msrc.am; ford@chem.ucsb.edu

Abstract: The reaction(s) of nitric oxide (nitrogen monoxide) gas with sublimed layers containing the nitrate iron(III) complex $\text{Fe}^{\text{III}}(\text{TPP})(\eta^2\text{-O}_2\text{NO})$ (**1**, TPP = *meso*-tetraphenyl porphyrinate²⁻) leads to formation of several iron porphyrin species that are ligated by various nitrogen oxides. The eventual products of these low-temperature solid-state reactions are the nitrosyl complex $\text{Fe}(\text{TPP})(\text{NO})$, the nitro-nitrosyl complex $\text{Fe}(\text{TPP})(\text{NO}_2)(\text{NO})$, and **1** itself, and the relative final quantities of these were functions of the NO partial pressure. It is particularly notable that isotope labeling experiments show that the nitrate product is not simply unreacted **1** but is the result of a series of transformations taking place in the layered material. Thus, the nitrate complex formed from solid $\text{Fe}(\text{TPP})(\eta^2\text{-O}_2\text{NO})$ maintained under a ¹⁵N₂O atmosphere was found to be the labeled analogue $\text{Fe}(\text{TPP})(\eta^2\text{-O}_2\text{-}^{15}\text{NO})$. The reactivities of the layered solids are compared to the behaviors of the same species in ambient temperature solutions. To interpret the reactions of the labeled nitrogen oxides, the potential exchange reactions between N₂O₃ and ¹⁵NO were examined, and complete isotope scrambling was observed between these species under the reaction conditions (*T* = 140 K). Overall it was concluded from isotope labeling experiments that the sequence of reactions is initiated by reaction of **1** with NO to give the nitrate nitrosyl complex $\text{Fe}(\text{TPP})(\eta^1\text{-ONO}_2)(\text{NO})$ (**2**) as an intermediate. This is followed by a reaction in the presence of excess NO that is equivalent to the loss of the nitrate radical NO₃[•] to give $\text{Fe}(\text{TPP})(\text{NO})$ as another transient species. A plausible pathway involving NO attack on the coordinated nitrate of **2** resulting in the release of N₂O₄ concerted with electron transfer to the metal center is proposed.

Introduction

Nitric oxide (NO) has been well-characterized as an important regulatory molecule in mammalian biology. The interaction of NO with ferro- and ferri-*heme* proteins plays a central role in this bioregulatory activity,¹ and the reactions of NO with various iron porphyrin complexes have been investigated as models for these processes.² In addition to simple association reactions, NO has been shown to participate in reversible redox reactions involving biologically relevant metal centers. In model reactions it is clear that metal complexes mediate both oxygen atom and electron-transfer processes involving NO and various other nitrogen oxide species (NO_x). Such oxidative processes may not only be significant in the biological chemistry of various NO_x but also have potential in the catalytic oxidations of various organic substrates.³ It was in these contexts that the present study was initiated, with the goal of elucidating the redox transforma-

tions between various NO_x complexes of the *heme* model compound $\text{Fe}(\text{TPP})$ (TPP = *meso*-tetraphenyl porphyrinate²⁻) using the bidentate nitrate complex $\text{Fe}(\text{TPP})(\eta^2\text{-O}_2\text{NO})$ (**1**)⁴ as the entry point. This compound can be prepared by reaction of the oxo-bridged $[\text{Fe}(\text{TPP})]_2\text{O}$ with HNO₃,⁴ and it has also been shown to be a product of the NO₂ reactions with $\text{Fe}(\text{TPP})$ species both in the solid state and in solutions.^{5,6}

The present investigations were carried out both in solution and in sublimed layers of the iron porphyrin complex using infrared and electronic spectroscopic probes of the transformations. The low-temperature spectral investigations of the sublimed layers provide the opportunity to observe the stepwise reactions that lead to the formation of the final products and to

- (3) (a) Tovrog, B. S.; Mares, F. M.; Diamond, S. E. *J. Am. Chem. Soc.* **1980**, *102*, 6616–6618. (b) Andrews, M. A.; Chang, T.; Cheng, C.-W. *Organometallics* **1985**, *4*, 268–274. (c) Castro, C. E. *J. Org. Chem.* **1996**, *61*, 6388–6395. (d) Goodwin, J., et al. *Inorg. Chem.* **2001**, *40*, 4217–4225.
- (4) Phillippi, M. A.; Baenziger N.; Goff, H. M. *Inorg. Chem.* **1981**, *20*, 3904–3911.
- (5) Kurtikyan, T. S.; Stepanyan, T. G.; Akopyan, M. E. *Russ. J. Coord. Chem.* **1999**, *25*, 721–725.
- (6) (a) Kurtikyan, T. S.; Martirosyan, G. G.; Lorkovic', I. M.; Ford, P. C. *J. Am. Chem. Soc.* **2002**, *124*, 10124–10129. (b) Lim, M. D.; Lorkovic, I. M.; Wedeking, K.; Zanella, A. W.; Massick, S. M.; Ford, P. C. *J. Am. Chem. Soc.* **2002**, *124*, 9737–9743.

[†] Research Institute of Applied Chemistry.

[‡] Molecule Structure Research Centre NAS.

[§] University of California.

(1) Ignarro, L. *Nitric Oxide: Biology and Pathobiology*; Academic Press: San Diego, CA, 2000.

(2) Ford, P. C.; Lorkovic, I. M. *Chem. Rev.* **2002**, *102*, 993–1017.

characterize the intermediates that define these transformations. The solution studies offer the opportunity to evaluate whether such reactions follow analogous pathways in fluid media and to observe the dynamics of these processes.

Experimental Section

Preparation of Fe(TPP)(η^2 -O₂NO) Sublimates. Fe(II) porphyrinates are very sensitive to oxygen and readily transform to Fe(III) derivatives. For this reason, the more stable Fe(TPP)(B)₂ complexes with nitrogen bases (B is pyridine or piperidine) were used as parent compounds. These were synthesized by a known procedure.⁷ The low-temperature sublimate was prepared⁸ by placing an Fe(TPP)(B)₂ sample in a Knudsen cell and heating to about 470 K under high vacuum ($P = 3 \times 10^{-5}$ Torr). Evacuation for 3 h resulted in the complete elimination of the coordinated axial ligands B, as monitored by measurement of the pressure at the outlet of the cryostat. Liquid nitrogen was then poured into the cryostat, and the Knudsen cell was heated to 520 K, at which temperature sublimation of Fe(TPP) onto the KBr and CaF₂ substrate occurred. In the latter case, CaF₂ plates were also used as the optical windows of the cryostat.^{9,10} The M(TPP) layers obtained in this manner by sublimation onto a low-temperature (77 K) surface are spongelike and have high microporosity.¹¹ Potential reactants easily diffuse across these layers, and adducts thus formed can be studied spectroscopically without solvent interference.

Sublimation was typically carried out over periods of 0.1–2.0 h to build up layers of thickness convenient for UV–visible and IR spectral studies. The Fe(TPP) sublimed layer was heated to room temperature under dynamic vacuum, and then NO₂ gas was introduced. As shown previously,⁵ this procedure leads to the formation of a very clean spectrum of the bidentate nitrate complex **1**. These layers were then cooled with liquid nitrogen, and NO was fed to the cryostat from a vessel provided with a mercury manometer to measure the pressure of NO. The layers were warmed to specified temperatures controlled by thermocouple, and FTIR or electronic absorption spectra were measured.

Labeled and Unlabeled Nitric Oxide. NO gas was purified by passage through KOH pellets and a cold trap (dry ice/acetone) to remove higher nitrogen oxides and trace quantities of water. The purity was checked by IR measurements of the layer obtained by slow deposition of NO on the cooled substrate of the optical cryostat (80 K), which did not show the characteristic IR bands of N₂O, N₂O₃, or H₂O, thus indicating the absence of these species. (Freezing the purified NO with the liquid nitrogen on the wall of the glass storage bulb serves as a rapid procedure for checking purity, since in the presence of NO₂, this solid takes on the bluish color from the trace N₂O₃.) ¹⁵N with 98.5% enrichment was purchased from the Institute of Isotopes, Republic of Georgia, and was purified by the same procedures. NO₂ (¹⁵NO₂), obtained by oxidation of NO (¹⁵NO) with excess of pure dioxygen, was dried over P₂O₅ and then was purified by fractional distillation until a pure white solid was obtained.

Solution Studies. Solid Fe(TPP)(η^2 -O₂NO) (**1**) was prepared following a published procedure⁴ and was stored in an inert atmosphere glovebox. Solutions were prepared in the glovebox using distilled and deoxygenated solvents and then loaded into gastight syringes for transfer to the reaction cells. NO was purified, measured, and transferred

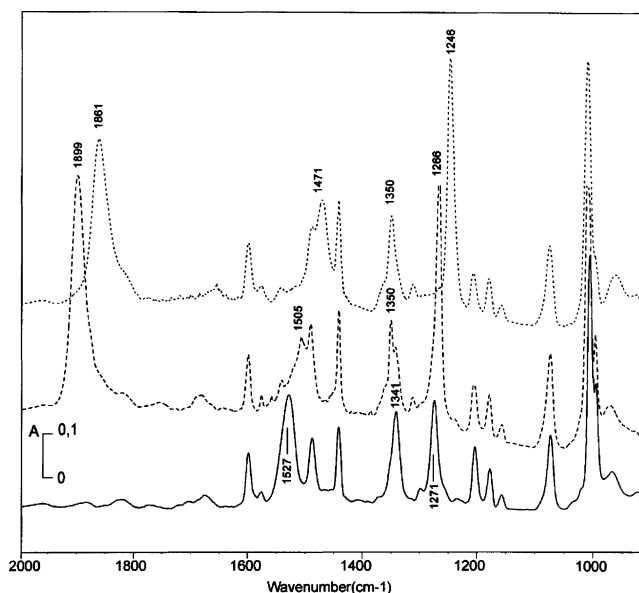


Figure 1. Low-temperature (80 K) FTIR spectra of (a) a thin film of Fe(TPP)(η^2 -O₂NO) (solid line), (b) after supplying 10 Torr NO to cryostat at 80 K followed by warming to 140 K, pumping briefly to remove excess NO and recoiling to 80 K (dashed line), (c) the same after interaction of ¹⁵N with Fe(TPP)(η^2 -O₂¹⁵NO) (dotted line).

quantitatively using vacuum line techniques directly into an airtight flask that included a 1.0-cm quartz cuvette for monitoring reactions via changes in their UV–visible spectra. A typical reaction would be initiated by injection of the porphyrin solution into this reaction vessel, shaken vigorously to provide gas/solution equilibration, and then mounting the cuvette in the spectrophotometer. The electronic spectra were acquired at 10-s intervals for the initial 200 s and at longer time increments afterward.

Infrared spectra of reacting solutions were recorded using rapid mixing techniques with a custom-made instrument. Two gastight syringes were connected via PEEK tubing to a mixing block that preceded the entrance to a 0.5-mm CaF₂ IR cell. Before use, the apparatus was evacuated overnight under vacuum. Purified NO was transferred using vacuum line techniques into a sealed glass flask and brought into the glovebox where degassed CH₂Cl₂ was injected into the NO-containing flask. The equilibrated solution was then loaded directly into one of the gastight syringes. The second syringe was filled with a CH₂Cl₂ solution of **1**. A mechanical device was used to engage the two syringes simultaneously, causing the solutions to mix and flow to an IR cell mounted in an FTIR spectrometer. The first acquisition was taken while the syringe driver was running, and spectra were acquired after this was disengaged and the exit valve was closed.

Instrumentation. FTIR spectra of porphyrin sublimates were obtained on Nicolet Nexus FTIR and Specord M-80 spectrometers, and electronic spectra were recorded on a Specord M-40 spectrophotometer. Solution kinetics studies were carried out on an HP 8452 diode array spectrophotometer or on a modernized BioRad model FTS-Pro FTIR spectrophotometer.

Results and Discussion

Formation of Fe(TPP)(η^1 -ONO₂)(NO) (2**) in Low-Temperature Films.** The nitrate nitrosyl complex **2** represents the only characterized example of a six-coordinate nitrate ferro or ferri-porphyrinato complex. This was described several years ago in a preliminary communication¹² and is described in greater detail here. Figure 1 presents the FTIR spectra of the product

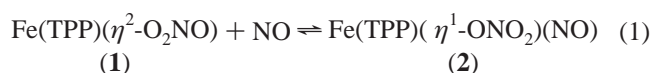
- (7) Epstein, L. M.; Straub, D. K.; Maricondi, C. *Inorg. Chem.* **1967**, *6*, 1720–1722.
 (8) Nakamoto, K.; Watanabe, T.; Ama, T.; Urban, M. W. *J. Am. Chem. Soc.* **1982**, *104*, 3744–3745.
 (9) Experiments using CaF₂ optics were performed to avoid additional bands that appear in the 1350 cm⁻¹ region due to interaction of NO₂ gas with salt windows.¹⁰
 (10) Peters, S. J.; Ewing, G. E. *J. Phys. Chem.* **1996**, *100*, 14093–14102.
 (11) (a) Byrn, M. P.; Curtis, C. J.; Hsiou, Y.; Khan, S. I.; Sawin, P. A.; Tendick, S. K.; Terzis, A.; Strouse, C. E. *J. Am. Chem. Soc.* **1993**, *115*, 9480–9497. (b) Byrn, M. P.; Curtis, C. J.; Khan, S. I.; Sawin, P. A.; Tsurumi, R.; Strouse, C. E. *J. Am. Chem. Soc.* **1990**, *112*, 1865–1874. (c) Kurtikyan, T. S.; Gasparyan, A. V.; Martirosyan, G. G.; Zhamkochyan, G. H. *J. Appl. Spectrosc. (Russ.)* **1995**, *62*, 62–66.

- (12) Kurtikyan, T. S.; Martirosyan, G. G.; Hakobyan, M. E.; Ford, P. C. *Chem. Commun.* **2003**, 1706–1707.

Table 1. IR Spectral Data of Nitrosyl and Nitrate Groups for Fe(TPP)(ONO₂)(NO) in cm⁻¹

Fe(TPP)(ONO ₂)(NO)	Fe(TPP)(ONO ₂)(¹⁵ NO)	Fe(TPP)(O ¹⁵ NO ₂)(NO)	Fe(TPP)(O ¹⁵ NO ₂)(¹⁵ NO)	assignment
1899 s	1862 s	1900 s	1863 s	$\nu(\text{N}=\text{O})$
1505 m	1505 m	1472 m	1472 m	$\nu_a(\text{NO}_2)$
1265 s	1265 s	1246 s	1246 s	$\nu_s(\text{NO}_2)$
969 w	969 w	954 w	954 w	$\nu(\text{N}-\text{O})$
605 vw	602 vw	605 vw	602 vw	$\delta(\text{Fe}-\text{N}-\text{O})$
548 vw	542 vw	548 vw	542 vw	$\nu[\text{Fe}-\text{N}(\text{NO})]$

obtained after exposing a low-temperature (80 K) layer of solid Fe(TPP)(η^2 -O₂NO) to NO gas, warming to 140 K, pumping out the excess NO, and then recooling. The transformation is characterized by appearance of new bands at 1899 s, 1506 m, 1265 s, and 969 w cm⁻¹ and disappearance of bands at 1528 and 1273 cm⁻¹ attributed to bidentate-coordinated nitrate. Additionally, a porphyrin band at 1341 cm⁻¹ is shifted to 1350 cm⁻¹, while new weak bands at 605, 548, and 464 cm⁻¹ appear at low frequency (Supporting Information Figure S1). The intensities of the new bands correlate during their growth (Supporting Information Figure S2) and can be confidently assigned to the formation of **2** as depicted in eq 1.



When the same procedure is carried out with the isotopically labeled materials ¹⁵NO and Fe(TPP)(η^2 -O₂¹⁵NO), the new bands appear at the shifted frequencies 1863 s, 1472 m, 1246 s, 954 w, 602 vw, and 542 vw cm⁻¹ (Figure 1, dotted line), but others at 1350 and 464 cm⁻¹ are not affected by the isotope labeling. If instead the reaction is between ¹⁵NO gas and unlabeled **1**, the product spectrum displays bands at 1862 s, 1505 m, 1265 s, 969 w, 602 vw, and 542 vw cm⁻¹ (Supporting Information Figure S3), that is, only the new bands at 1862, 602, and 542 cm⁻¹ are shifted relative to the product bands seen in the reaction between unlabeled NO and **1** shown in Figure 1. When this procedure was performed with unlabeled NO and Fe(TPP)(O₂¹⁵-NO), the IR spectrum displayed bands at 1900 s, 1472 m, 1246 s, 954 w, 605 vw, and 548 vw cm⁻¹ (Supporting Information Figure S3) where only those at 1900, 605, and 548 cm⁻¹ are unchanged relative to the unlabeled reaction. Spectral data obtained for these systems are summarized in Table 1. These results indicate that, in the 80–140 K temperature interval, the only observable reaction proceeding in the layer is addition of NO to Fe(TPP)(η^2 -O₂NO) (**1**) to give the six-coordinate complex Fe(TPP)(η^1 -ONO₂)(NO) (**2**).

The electronic absorption spectra recorded under identical conditions and using CaF₂ optics as used to record the FTIR spectra with the same sample also demonstrated formation of the new complex. The Soret band of **1** in the 80 K thin film appears at 423 nm, about 10 nm red-shifted from that seen in the ambient temperature solution spectrum of **1**, but the Q-bands at 511 and 572 nm are close to the reported solution values.^{4,13} Upon addition of NO gas, the optical spectrum (Figure 2, dashed line) is significantly changed. The Soret and Q-bands of the new species are shifted to higher wavelengths (436, 547 and 582 nm) as illustrated in Figure 2 (solid line). Notably, this spectrum is similar to that of other hexacoordinate Fe^{III}

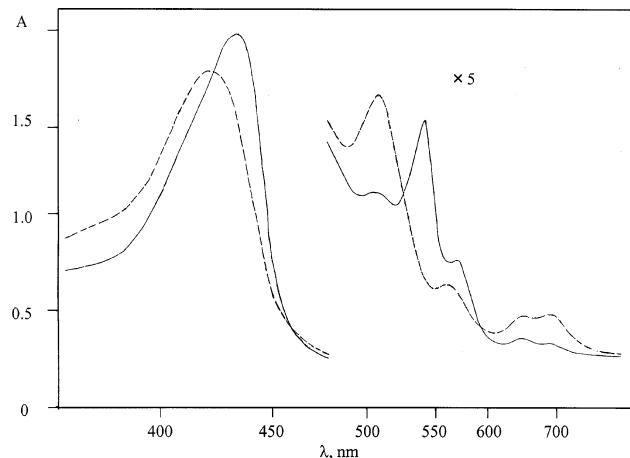


Figure 2. (a) Low-temperature (80 K) UV–visible spectrum of a sublimed layer of Fe(TPP)(η^2 -O₂NO) (dashed line). (b) Optical spectrum after exposing **1** to NO (5 Torr at 77 K warming to 140 K and recooling) (solid line).

porphyrin complexes of mixed nitrogen oxides. For example, the electronic spectrum of the nitro nitrosyl complex Fe(TPP)(NO₂)(NO) (**3**) in chloroform solution displays a spectrum with maxima at 433, 545, and 577 nm.¹⁴

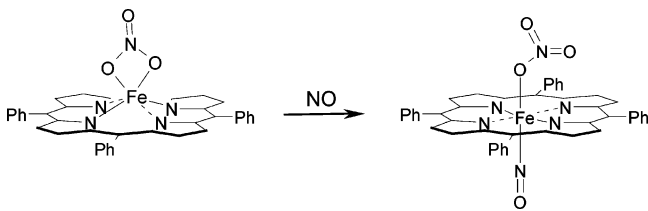
The bidentate nitrate ligand of Fe(TPP)(η^2 -O₂NO) (**1**) has been shown to be bound in a slightly asymmetric mode with a large out-of-plane displacement (0.6 Å) of the d⁵ high-spin Fe(III) center toward the lone axial ligand.⁴ For this structure, the η^2 -nitrate ligand would be expected to show three IR-active stretching modes, a high-frequency $\nu(\text{N}=\text{O})$ stretch for the uncoordinated oxygen, and symmetric and asymmetric stretching modes for the coordinated NO₂ fragment. Two bands of compatible intensity seen for **1** at 1530 and 1275 cm⁻¹ in Nujol mull⁴ and in sublimed layers⁵ were assigned, respectively, to $\nu(\text{N}=\text{O})$ and to the asymmetric mode of the coordinated NO₂ fragment.¹⁵ The low-intensity, but isotopically sensitive, FTIR band near 965 cm⁻¹ (Figure S3) can plausibly be assigned to the symmetric stretching mode of the NO₂ fragment of **1**.¹⁵

Adding NO to samples of **1** shifts the high-frequency vibrations of coordinated nitrate to lower frequencies with a change in the relative intensities, the higher energy band diminishing and the lower energy band becoming much stronger. Additionally there is enhancement and shift of the weak symmetric stretching mode of the NO₂ fragment. These changes can be interpreted in terms of the bidentate-to-monodentate transition of the nitrate coordination illustrated by Scheme 1. The highest-frequency nitrate band at 1505 cm⁻¹ now represents $\nu_a(\text{NO}_2)$, while that at ~1260 cm⁻¹ is assigned to $\nu_s(\text{NO}_2)$. For comparison, the IR spectrum of the monodentate nitrate complex Fe(OEP)(η^1 -ONO₂) (OEP = octaethylporphyrinato²⁻) displays

(13) The UV–vis spectrum of the film sample dissolved in CH₂Cl₂ is quite similar to reported solution data;⁴ hence the red shift of Soret band is evidently a solid-state effect.

(14) Yoshimura, T. *Inorg. Chim. Acta* **1984**, *83*, 17–21.

(15) Nakamoto, K. *Infrared and Raman Spectra of Inorganic and Coordination Compounds*, 3rd ed.; Wiley: New York, 1978; pp 244–247.

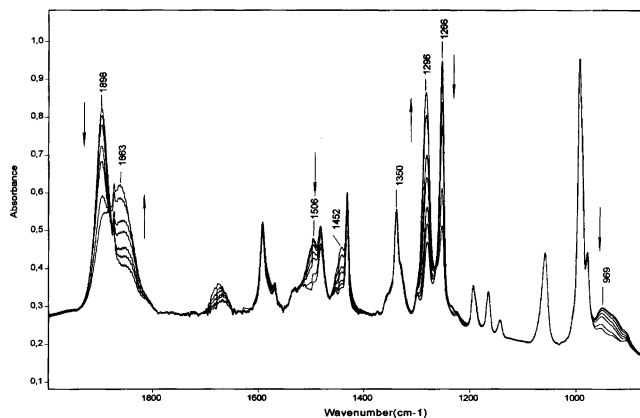
Scheme 1. Schematic Representation of the Reaction between Fe(TPP)(NO₃) and NO

a coordinated nitrate band at 1515 cm^{-1} (KBr pellet).¹⁶ Closer disposition of the high-frequency bands is one criterion of monodentate coordination in nitrate complexes.¹⁵ The band at $\sim 970\text{ cm}^{-1}$ can be assigned to the N–O vibration for the coordinated oxygen.

The low-frequency weak bands at 605 (602) and 548 (542 cm^{-1}) sensitive to NO labeling should be assigned to metal-nitrosyl vibrations. The former was tentatively assigned to δ -(Fe–N–O), while the latter to ν (Fe–N) by analogy with Fe(III)(tropocoronand)(nitrosyl) complex,¹⁷ in which deformation Fe–N–O mode of linearly bound NO is disposed at higher frequencies and revealed smaller isotopic shift than Fe–N stretching.

Additional information regarding the nature of **2** can be drawn from porphyrin vibrational modes that reveal systematic changes depending on the spin and oxidation states of axial complexes of Fe(TPP).¹⁸ The band in vicinity of 1350 cm^{-1} representing a porphyrin core mode (ν (C_a–C_m) mixed with some ν (C_m–phenyl)) lies at higher frequencies in low-spin complexes. Similarly, a low-energy porphyrin core deformation mode occurs in the range 450 cm^{-1} . For the high-spin η^2 -nitrate complex **1**, these bands lie at 1341 and 436 cm^{-1} . Upon coordination of NO, they shift to 1350 and 464 cm^{-1} (see Figures 1 and S1), indicating a change to the low-spin state. This result is consistent with other low-spin, six-coordinate ferri-heme nitrosyl complexes¹⁹ and supports the conclusion that, under these conditions, NO reacts with Fe(TPP)(η^2 -O₂NO) to give Fe(TPP)(η^1 -ONO₂)(NO). While this bidentate-to-monodentate transition may alleviate nonbonded repulsions between nitrate oxygens and porphyrin nitrogens, it is likely to involve relatively moderate energy expenditures given the existence of monodentate and bidentate binding, respectively, in Fe(OEP)(ONO₂) and Fe(TPP)(O₂NO), which differ only in the nature of the peripheral substituents. To our knowledge, the only other six-coordinate nitrate Fe(P) complex known is an aqua complex (Fe(P)(η^1 -ONO₂)(H₂O)) (P not identified) reported in a review by Wyllie and Scheidt.¹⁹

Notably, ambient temperature solution studies described below also indicate the formation of **2** as an intermediate in the reaction of **1** with NO, although the former is unstable toward decay to other products. This behavior is in contrast to the greater stability of the analogous ruthenium complex Ru(TTP)(ONO₂)(NO) (TTP = *meso*-tetra(4-tolyl)porphyrinate dianion), which was first prepared by the solution reaction of Ru(TTP)(NO)Cl with AgNO₃²⁰ and subsequently by the reaction of Ru(TTP)(CO) with NO₂/N₂O₄.²¹

**Figure 3.** Formation of nitro nitrosyl complex Fe(TPP)(NO₂)(NO) from nitrate nitrosyl complex Fe(TPP)(η^1 -ONO₂)(NO) during the course of warming the sublimed layers from 145 to 180 K in the presence of NO (4 Torr).

Low-Temperature Reactions of Fe(TPP)(ONO₂)(NO) with NO. Transformations of solid Fe(TPP)(O₂NO) in thin films under a NO atmosphere can be divided into three temperature-dependent processes. At very low temperatures (80–140 K), the only process is the formation of nitrate nitrosyl complex **2**. Raising the temperature into the 140–200 K range leads to the further reaction of NO with this species, as illustrated in Figure 3. Warming of the layered material, in which **2** has been formed, leads to gradual intensity decreases in its characteristic bands at 1899, 1506, 1266, and 969 cm^{-1} , while new bands at 1863, 1452, and 1296 cm^{-1} gain intensity. The latter indicate the formation of the well-known nitro nitrosyl complex Fe(TPP)(NO₂)(NO) (**3**).^{6,14}

Further warming to room temperature is accompanied with partial reformation of the nitrate complex **1** and the appearance of the iron(II) nitrosyl complex Fe(TPP)(NO) (**4**). At this stage, the reactions are sensitive to the partial pressure of NO, and depending on P_{NO} , different relative quantities of **1**, **3**, and **4** are formed. At relatively high P_{NO} (a few decades of Torr), **3** is the main species seen in the solid layer, while at lower P_{NO} (a few Torr) all three are present in comparable amounts. Continuous evacuation to remove the headspace gases shifts the product mixture from Fe(TPP)(NO₂)(NO) to give increased yields of Fe(TPP)(O₂NO) and Fe(TPP)(NO).⁶

Scheme 2 offers several scenarios as starting points for discussing the reactions following exposing sublimed layers of Fe(TPP)(O₂NO) to NO gas. In each case, the first stage is formation of the nitrate nitrosyl complex **2** as evidenced from the low-temperature solid-state FTIR and by rapidly mixing UV–visible measurements in solution (see below). Three different pathways may be considered in evaluating the second stage of the reaction leading to Fe(TPP)(NO₂)(NO). Scenario (i) suggests that this is initiated by β -bond cleavage of NO₂ from **2** to give an oxo nitrosyl complex Fe^{IV}(TPP)(O)(NO), scenario (ii) involves oxygen atom abstraction from the coordinated nitrate ligand by excess NO to give directly a species of the same stoichiometry (but perhaps a linkage isomer) as **3** and NO₂, and scenario (iii) would be initiated by dissociation of an *NO₃ radical (perhaps assisted by reaction with NO) to give directly **4**, which is then rapidly oxidized to **3** by reaction with the NO₂ resulting from reaction of NO₃ with NO.²⁵

(16) Ellison, M. K.; Shang, M.; Kim, J.; Scheidt, W. R. *Acta Crystallogr., Sect. C* **1996**, C52, 3040–3043.

(17) Franz, K. J.; Lippard, S. J. *J. Am. Chem. Soc.* **1999**, 121, 10504–10512.

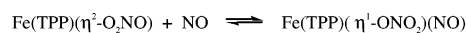
(18) Oshio, H.; Ama, T.; Watanabe, T.; Kincaid, J.; Nakamoto, K. *Spectrochim. Acta* **1984**, 40A, 863–870.

(19) Wyllie, G. R. A.; Scheidt, W. R. *Chem. Rev.* **2002**, 102, 1067–1089.

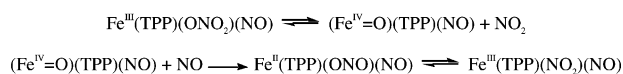
(20) Bohle, D. S.; Hung, C.-H.; Smit, B. D. *Inorg. Chem.* **1998**, 37, 5798–5806.

(21) Kang, Y.; Zyryanov, G. V.; Rudkevich, D. M. *Chem. Commun.* **2003**, 2470–2471.

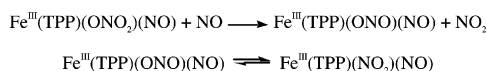
Scheme 2. Pathways for the Reactions of $\text{Fe}(\text{TPP})(\eta^2\text{-O}_2\text{NO})$ with Excess NO



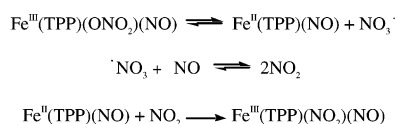
Scenario i (β -bond cleavage)



Scenario ii (Oxo-transfer from coordinated nitrate to free nitric oxide)



Scenario iii (elimination of nitrate radical)



IR measurements with isotopically labeled NO were used to lend insight into differentiating these pathways, with particular focus on the early stages before subsequent reactions lead to isotopic scrambling. For example, reaction of $\text{Fe}(\text{TPP})(\text{O}_2\text{NO})$ with excess ^{15}NO (system **A**) leads first to the formation of $\text{Fe}(\text{TPP})(\text{ONO}_2)(^{15}\text{NO})$, and different products are predicted for the subsequent reactions according to the three scenarios. Scenario (i) should give $\text{Fe}(\text{TPP})(^{15}\text{NO}_2)(^{15}\text{NO})$, scenario (ii) should give $\text{Fe}(\text{TPP})(\text{NO}_2)(^{15}\text{NO})$, and scenario (iii) should give a mixture of $\text{Fe}(\text{TPP})(^{15}\text{NO}_2)(^{15}\text{NO})$ and $\text{Fe}(\text{TPP})(\text{NO}_2)(^{15}\text{NO})$. Since all three are accompanied by formation of 1 mol of NO_2 , which in excess NO will give dinitrogen trioxide (N_2O_3), the appearance of the latter in the low-temperature spectrum would also be expected.

The results were as follows: Figure 4 (bottom) displays the FTIR spectral changes observed when excess ^{15}NO was added to $\text{Fe}(\text{TPP})(\text{O}_2\text{NO})$ (system **A**) to give $\text{Fe}(\text{TPP})(\text{ONO}_2)(^{15}\text{NO})$, and then the mixture was gradually warmed. The further reaction of $\text{Fe}(\text{TPP})(\text{ONO}_2)(^{15}\text{NO})$ is manifested by diminishing intensities of bands at 1860 (not shown), 1506, and 1266 cm^{-1} accompanied with the appearance of new bands at ~ 1830 (not shown), 1452, 1422, 1295, and 1273 cm^{-1} . The new bands at 1830, 1452, and 1295 cm^{-1} belong to the $\nu(^{15}\text{NO})$, $\nu_a(\text{NO}_2)$, and $\nu_s(\text{NO}_2)$ absorptions of $\text{Fe}(\text{TPP})(\text{NO}_2)(^{15}\text{NO})$, while those at 1422 and 1273 cm^{-1} can be assigned to $^{15}\text{NO}_2$ stretches of the doubly labeled complex $\text{Fe}(\text{TPP})(^{15}\text{NO}_2)(^{15}\text{NO})$. In the latter case, unambiguous assignment of the band at 1273 cm^{-1} is complicated, since $(^{15}\text{N})_2\text{O}_3$ also shows absorptions in the same region. IR bands at 1830, 1546, and 1277 cm^{-1} are reported for solid $(^{15}\text{N})_2\text{O}_3$.²² The growth of the weak band at ~ 1550 cm^{-1} confirms formation of $(^{15}\text{N})_2\text{O}_3$. These coincidences do not challenge the formation of $\text{Fe}(\text{TPP})(^{15}\text{NO}_2)(^{15}\text{NO})$ at this stage, since the band at 1422 cm^{-1} appears in a region relatively free of interference from the spectra of other NO_x species and of porphyrin itself. However, the bands at 1273 cm^{-1} (Figure

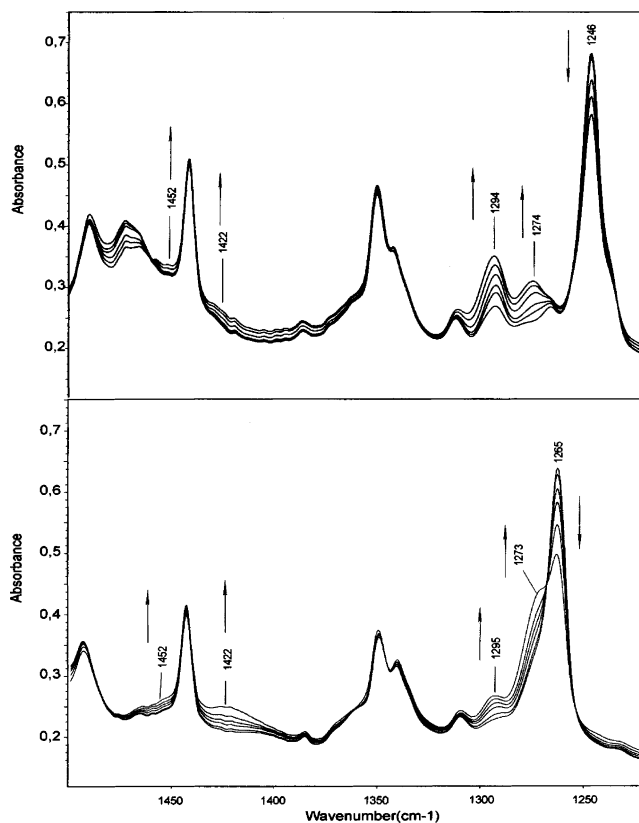


Figure 4. Isotope effects on FTIR spectra changes during the course of warming sublimed layers from 145 to 170 K in the presence of nitric oxide (4 Torr). Bottom: $^{15}\text{NO} + \text{Fe}(\text{TPP})(\text{NO}_3)$ (system **A**). Top: $\text{NO} + \text{Fe}(\text{TPP})(^{15}\text{NO}_3)$ (system **B**).

4, bottom) and in the vicinity of 1830 cm^{-1} may represent the overlapping absorptions characteristic of $\text{Fe}(\text{TPP})(^{15}\text{NO}_2)(^{15}\text{NO})$ and $(^{15}\text{N})_2\text{O}_3$.

Analogous data for addition of NO to $\text{Fe}(\text{TPP})(\text{O}_2^{15}\text{NO})$ (system **B**) to give initially $\text{Fe}(\text{TPP})(\text{O}^{15}\text{NO}_2)(\text{NO})$ are displayed in Figure 4 (top). The same analysis shows the disappearance of the latter to be accompanied by growth of bands at 1860 (not shown), 1452, 1422, 1296, and 1275 cm^{-1} . This can be interpreted in terms of the initial formation of two isotopomers: $\text{Fe}(\text{TPP})(\text{NO}_2)(\text{NO})$ (bands at 1860, 1452, and 1296 cm^{-1}) and $\text{Fe}(\text{TPP})(^{15}\text{NO}_2)(\text{NO})$ (bands at 1860, 1422, and 1275 cm^{-1}). Simultaneously, a weak band in the vicinity of 1590 cm^{-1} appears (due to N_2O_3) and enhances the intensity of the porphyrin band disposed in this region. Other bands characteristic of solid N_2O_3 appear at 1863 and 1297 cm^{-1} ,²² and they overlap with bands assigned to $\text{Fe}(\text{TPP})(\text{NO}_2)(\text{NO})$.

Interpretation of Isotope Studies of the Low-Temperature Reaction of 2 with NO. To a first approximation, these data appear to be consistent with scenario (iii) and not with (i) or (ii). For example, scenario (i) predicts that system **A** would give $\text{Fe}(\text{TPP})(^{15}\text{NO}_2)(^{15}\text{NO})$ and singularly labeled dinitrogen trioxide ($\text{O}^{15}\text{NNO}_2$) and system **B** to give $\text{Fe}(\text{TPP})(\text{NO}_2)(\text{NO})$ and $\text{ON}^{15}\text{NO}_2$.²³ In contrast, system **A** gave $\text{Fe}(\text{TPP})(\text{NO}_2)(^{15}\text{NO})$, $\text{Fe}(\text{TPP})(^{15}\text{NO}_2)(^{15}\text{NO})$, and $(^{15}\text{N})_2\text{O}_3$ while system **B** gave $\text{Fe}(\text{TPP})(\text{NO}_2)(\text{NO})$, $\text{Fe}(\text{TPP})(^{15}\text{NO}_2)(\text{NO})$, and N_2O_3 . Additionally, no new IR bands were found in the region where ferryl $\nu(\text{Fe}=\text{O})$ stretches are usually disposed (750–860 cm^{-1}).²⁴

(22) Hisatsune, I. C.; Devlin, J. P.; Wada, Y. *J. Chem. Phys.* **1960**, *30*, 714–719.

(23) Here we consider only the more stable N–N bonded form of N_2O_3 .

(24) Nakamoto, K. *J. Mol. Struct.* **1997**, *408/409*, 11–16.

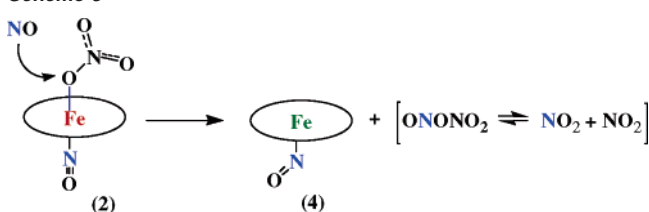
The situation is more ambiguous with regard to scenario (ii), which predicts system **A** formation of $(^{15}\text{N})_2\text{O}_3$ and $\text{Fe}(\text{TPP})\text{-(NO}_2\text{)}(^{15}\text{NO})$ (after isomerization of the initially formed nitrito complex) and system **B** formation of $\text{Fe}(\text{TPP})(^{15}\text{NO}_2)(\text{NO})$ and N_2O_3 . For each set of reaction conditions, products not predicted by scenario (ii) were formed, $\text{Fe}(\text{TPP})(^{15}\text{NO}_2)(^{15}\text{NO})$ in system **A** and $\text{Fe}(\text{TPP})(\text{NO}_2)(^{15}\text{NO})$ in system **B**.

As outlined in greater detail in Supporting Information Scheme S1, scenario iii predicts the formation of $\text{Fe}(\text{TPP})(^{15}\text{NO}_2)(^{15}\text{NO})$, $\text{Fe}(\text{TPP})(\text{NO}_2)(^{15}\text{NO})$, and both doubly and singly labeled dinitrogen trioxide for the conditions of system **A**, and $\text{Fe}(\text{TPP})(^{15}\text{NO}_2)(\text{NO})$, $\text{Fe}(\text{TPP})(\text{NO}_2)(\text{NO})$, and both singly labeled and unlabeled dinitrogen trioxide for the conditions of system **B**. The experimental results obtained are in agreement with scenario iii with the exception that only one type of dinitrogen trioxide was observed under each set of conditions, namely $(^{15}\text{N})_2\text{O}_3$ for system **A** and N_2O_3 for system **B**. A possible explanation of this inconsistency would be isotopic scrambling of the monolabeled species $\text{O}^{15}\text{NNO}_2$ and $\text{ON}^{15}\text{NO}_2$ by reaction with the excess nitric oxide present (^{15}NO in system **A** and NO in system **B**). This would give dinitrogen trioxide with the same nitrogen labeling as the added nitric oxide (^{15}NO and NO , respectively). This process should be facilitated by the formation of dinitrogen trioxide species isomers at very low temperatures.²⁶ Consistent with this point of view is the absence of published data describing the mixed isotope species as $\text{O}^{15}\text{NNO}_2$ or $\text{ON}^{15}\text{NO}_2$.

The possible exchange reaction between NO and N_2O_3 was examined under closely related experimental conditions using amorphous $\text{Ni}(\text{TPP})$ layers as adsorbent.²⁷ Partly oxidized NO was deposited on the $\text{Ni}(\text{TPP})$ layer at 80 K and warmed to 120 K, and then the system was evacuated to expel any free NO and then cooled back to 80 K. This procedure led to the formation of N_2O_3 which was manifested by IR bands at 1842, 1593, and 1292 cm^{-1} and a small amount of N_2O_4 in the layer with weak IR bands at 1734 and 1254 cm^{-1} .²² ^{15}NO was then introduced into the cryostat, and the FTIR spectra of this system were measured at various temperatures upon slow warming. This procedure showed that isotope exchange reaction occurs at temperatures as low as 140 K. Thus, under the experimental conditions used in the NO reaction with **2** to give **3**, the suggested isotopic exchange reaction should indeed lead to formation of dinitrogen trioxide species dominated by the isotopic composition of the excess nitric oxide.

Hence, of the three scenarios described by Scheme 2, the most plausible appears to be scenario iii, which is represented as initiating by elimination of a $\bullet\text{NO}_3$ radical (however, see the discussion below). Beside the experimental results given above, there is additional, indirect evidence consistent with this scenario. During the course of the reaction of $\text{Fe}(\text{TPP})(\text{ONO}_2)(\text{NO})$ (**2**) with NO to give $\text{Fe}(\text{TPP})(\text{NO}_2)(\text{NO})$ (**3**), a weak band in the vicinity of 1675 cm^{-1} initially grows and then diminishes in intensity (Figure 3). This can be interpreted in terms of formation and decay of $\text{Fe}(\text{TPP})(\text{NO})$ (**4**) as an intermediate resulting from $\bullet\text{NO}_3$ elimination.

Scheme 3



The fundamental problem with scenario iii is that the $\bullet\text{NO}_3$ radical is a high energy species,²⁸ and although its formation from **2** should be facilitated by the high thermodynamic stability of **4**, the first step in this sequence would appear to be substantially uphill. However, an alternative step by which the loss of an $\bullet\text{NO}_3$ equivalent might be effected would be the direct reaction of the excess NO with the coordinated nitrate ligand. In effect, this is equivalent to the reductive nitrosation of a coordinated ligand identified recently with a copper(II) complex²⁹ in the context that the coordinated anion is nitrosated concomitant with the reduction of the metal center (in this case the reduced metal species is **4**) as illustrated in eq 2. With $\text{X}^- = \text{nitrate}$ and $\text{L}_m\text{M}^{n+} = \text{Fe}(\text{TPP})(\text{NO})$, the concerted transfer of a NO_3 equivalent to NO to give some form of N_2O_4 and the very stable **4** as intermediates would give the same product distributions as scenario iii while avoiding the formation of the very high energy nitrate radical.



Hence, we believe that the most plausible mechanism for formation of $\text{Fe}(\text{TPP})(\text{NO}_2)(\text{NO})$ (**3**) from **2** involves the pathway represented in Scheme 3. Reaction of NO_2 with the nitrosyl complex **4** would rapidly give **3**.⁶ Notably, the reaction of NO with coordinated nitrate to give an ONONO_2 species is the microscopic reversal of a likely first step in the formation of $\text{Ru}(\text{TTP})(\text{ONO}_2)(\text{NO})$ by the reaction of N_2O_4 with $\text{Ru}(\text{TTP})(\text{CO})$.²¹

Higher Temperature Reactions of $\text{Fe}(\text{TPP})(\text{NO}_x)$ Films with NO . For system **A**, further warming of the layer does not significantly change the intensity of the 1296 cm^{-1} band of $\text{Fe}(\text{TPP})(\text{NO}_2)(^{15}\text{NO})$, but the $\nu_s(^{15}\text{NO}_2)$ and $\nu_a(^{15}\text{NO}_2)$ bands (1275 and 1422 cm^{-1} , respectively) corresponding to the fully labeled nitro nitrosyl complex $\text{Fe}(\text{TPP})(^{15}\text{NO}_2)(^{15}\text{NO})$ grow more intense. An analogous pattern is observed for system **B** (excess NO) where the intensity of the $\nu_s(^{15}\text{NO}_2)$ band for $\text{Fe}(\text{TPP})(^{15}\text{NO}_2)(\text{NO})$ (1275 cm^{-1}) grows only to a certain level while intensities of the $\nu_s(\text{NO}_2)$ and $\nu_a(\text{NO}_2)$ bands of $\text{Fe}(\text{TPP})(\text{NO}_2)(\text{NO})$ (1296 and 1452 cm^{-1} , respectively) continue to increase. At the end of this stage of reaction, the layers consist mostly of $\text{Fe}(\text{TPP})(^{15}\text{NO}_2)(^{15}\text{NO})$ and $\text{Fe}(\text{TPP})(\text{NO}_2)(\text{NO})$ for experiments with excess ^{15}NO and NO , correspondingly. This process can be rationalized according to the hypothetical pathway presented in Scheme 4. Other mechanisms involving oxidation of coordinated NO by NO_2 , decomposition of a putative dinitro

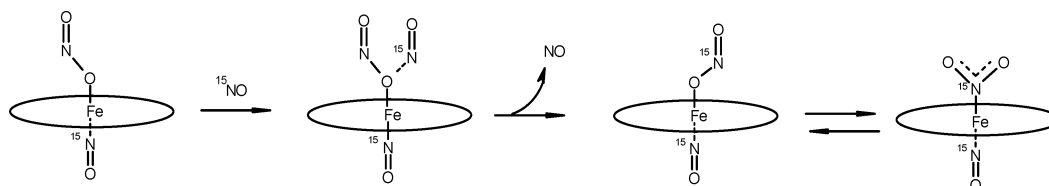
(25) Wayne, R. P., et al. *Atmos. Environ.* **1991**, 25A, 1–203.

(26) Fateley, W. G.; Bent, H. A.; Crawford, B. J. *Chem. Phys.* **1959**, 31, 204–217.

(27) (a) At low temperatures, sublimed layers of $\text{Ni}(\text{TPP})$ react with neither NO nor NO_2 , while at room temperature NO_2 oxidizes porphyrin ring with formation of $\text{Ni}(\text{TPP})^+(\text{NO}_2)^-$ ion pair.^{26b} (b) Martirosyan, G. G.; Kurtykian, T. S. *Zh. Prikl. Khim.* (Russ.) **1998**, 71, 1595–1598.

(28) (a) The electron affinity of the NO_3 radical has been reported^{27b} to be 375 kJ mol^{-1} . (b) Lias, S. G.; Barmes, J. E.; Holmes, J. L.; Levin, R. D.; Mallard, W. G. *J. Phys. Chem. Ref. Data* **1988**, 17 (Suppl. 1), 1–86 as summarized on p 43 in Huheey, J. E.; Keiter, E. A.; Keiter, R. L. *Inorganic Chemistry*, 4th ed.; Harper-Collins College Publishers: New York, 1993.

(29) (a) Tsuge, K.; DeRosa, F.; Lim, M. D.; Ford, P. C. *J. Am. Chem. Soc.* **2004**, 126, 6564–6565. (b) Ford, P. C.; Fernandez, B. O.; Lim, M. D. *Chem. Rev.*, published online Feb 18, 2005. <http://dx.doi.org/10.1021/CR0307289>.

Scheme 4. Possible Mechanism of Isotope Exchange for $\text{Fe}(\text{TPP})(\text{NO}_2)(^{15}\text{NO}) + ^{15}\text{NO}$ 

complex, and re-formation of isotopically exchanged **3** cannot be ruled out. Isotope mixing could also occur just by ligand exchange.

In contrast to the well-defined temperature interval that divides formation of the nitrate nitrosyl complex **2** from the subsequent transformation of **2** to the nitro nitrosyl complex **3**, there are no clear temperature boundaries between the latter processes and subsequent steps in these solid films leading to the partial formation of $\text{Fe}(\text{TPP})(\text{NO}_3)$ and $\text{Fe}(\text{TPP})(\text{NO})$. In the presence of NO, all three species, namely, **1**, **3**, and **4**, are formed in the layer in relative quantities depending on P_{NO} . Exhaustive evacuation of NO from the cryostat depleted **3** and increased quantities of **1** and **3**.

Isotopic experiments with systems **A** and **B** help elucidate reformation of $\text{Fe}(\text{TPP})(\text{O}_2\text{NO})$ during this stage (Figure 5). The bands that appear at 1245 cm^{-1} in system **A** and at 1265 cm^{-1}

in system **B** can be assigned, respectively, to formation of $\text{Fe}(\text{TPP})(^{15}\text{NO})(\text{O}^{15}\text{NO}_2)$ and $\text{Fe}(\text{TPP})(\text{ONO}_2)(\text{NO})$. Further warming of the layer is accompanied by decreases of these bands and increased intensities of new ones at 1253 and 1273 cm^{-1} corresponding to the appearance of $\text{Fe}(\text{TPP})(^{15}\text{NO}_3)$ and $\text{Fe}(\text{TPP})(\text{NO}_3)$. The well-defined isosbestic points seen in Figure 5 indicate that these spectral changes are coupled to the transformation of $\text{Fe}(\text{TPP})(\text{O}^{15}\text{NO}_2)(^{15}\text{NO})$ to $\text{Fe}(\text{TPP})(^{15}\text{NO}_3)$ (in **A**) and $\text{Fe}(\text{TPP})(\text{ONO}_2)(\text{NO})$ to $\text{Fe}(\text{TPP})(\text{NO}_3)$ (in **B**). Oddly, under these conditions, the processes described before appear to be reversed; that is, **3** is oxidized to the nitrate analogue **2**, which loses NO to regenerate **1**.

A plausible pathway for the oxidation of the coordinated nitro ligand would involve linkage isomerization of **3** to the nitrito analogue $\text{Fe}(\text{TPP})(\text{ONO})(\text{NO})$ (**5**) prior to oxygen transfer from one of the NO_x species present, probably NO_2 . There is only moderate spectral data regarding **5**, which was recently observed by irradiation of a KBr pellet containing $\text{Fe}(\text{TPP})(\text{NO}_2)(\text{NO})$ at low-temperature conditions.³⁰ In difference spectra, isotope-sensitive bands at 1507 and 934 cm^{-1} were assigned to $\nu(\text{N}=\text{O})$ and $\nu(\text{N}-\text{O})$ of coordinated nitrito ligand in six-coordinate nitrito nitrosyl complex $\text{Fe}(\text{TPP})(\text{ONO})(\text{NO})$. Similar isotope-sensitive bands at 1528 and 908 cm^{-1} were recorded in the course of low-temperature studies of the reaction between small quantities of NO_2 with sublimed layers of $\text{Fe}(\text{TPP})$ and were assigned to the same stretching modes as those in five-coordinate nitrito complex $\text{Fe}(\text{TPP})(\text{ONO})$.³¹ Close examination of the spectra presented in Figure 3 shows that the broad band in the vicinity of 970 cm^{-1} has a low frequency shoulder, suggesting the presence of an additional weak band with a maximum in the vicinity of 940 cm^{-1} . We believe that this isotope-sensitive band belongs to **5**, although bands in the vicinity of 1900 and 1500 cm^{-1} are obscured by those of $\text{Fe}(\text{TPP})(\text{ONO}_2)(\text{NO})$ (**2**).

Solution-Phase Reactivity Studies at Ambient Temperature. We have also briefly investigated the solution-phase reactions of $\text{Fe}(\text{TPP})(\text{O}_2\text{NO})$ (**1**) with NO at ambient temperature, and these gave spectral changes consistent with the chemical processes found in the solid films. The transformations after rapidly mixing solutions of **1** in toluene or dichloromethane and NO were followed by UV-vis and IR spectral measurements. Similar spectral changes were seen in both solvents. Figure 6 displays the changes in the electronic spectrum featuring the disappearance of **1** ($\lambda_{\text{Soret}} = 414\text{ nm}$, $\lambda_{\text{Q}} = 510\text{ nm}$) and the generation of a species with an electronic spectrum similar to that of $\text{Fe}(\text{TPP})(\text{NO}_2)(\text{NO})$ (**3**) ($\lambda_{\text{Soret}} = 432\text{ nm}$). Over a period of minutes the solution underwent further spectral changes to give a λ_{Soret} value at 406 nm , consistent with the formation of $\text{Fe}(\text{TPP})(\text{NO})$ (**4**). No simple $[\text{NO}]$ and $[\text{N}_2\text{O}_3]$

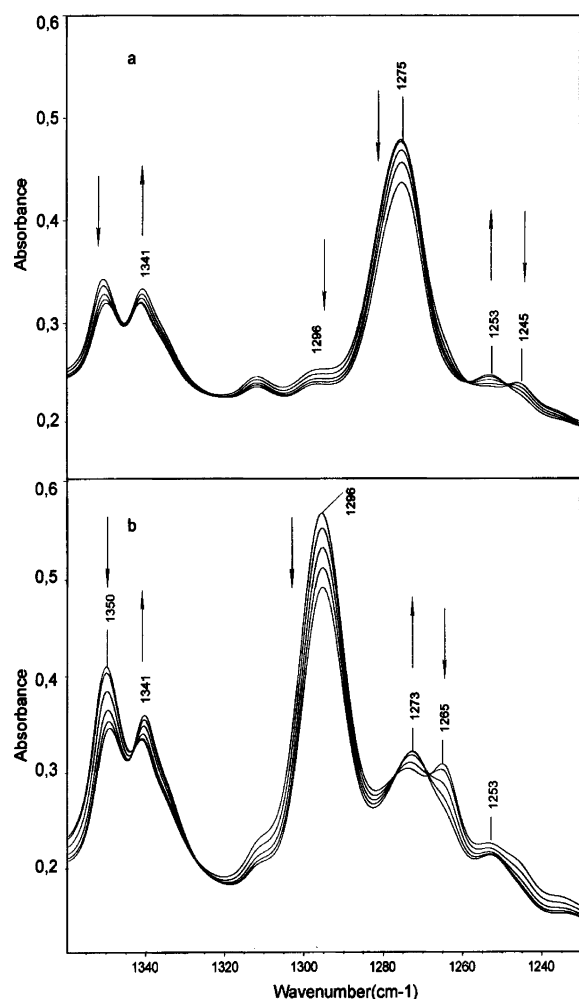


Figure 5. FTIR spectra changes resulting from warming sublimed layers from 200 to 240 K in the presence of nitric oxide (4 Torr). Bottom: $^{15}\text{NO} + \text{Fe}(\text{TPP})(\text{NO}_3)$ (system **A**). Top: $\text{NO} + \text{Fe}(\text{TPP})(^{15}\text{NO}_3)$ (system **B**).

(30) Lee, J.; Kovalevsky, A. Y.; Novozhilova, I.; Bagley, K.; Coppens, P.; Richter-Addo, G. B. *J. Am. Chem. Soc.* **2004**, *126*, 7180–7181.

(31) Kurtikyan, T. S.; Gulyan, G. M.; Ford, P. C. *Book of Abstracts*; XVI All-Russian Symposium on Modern Chemical Physics, Tuapse, Russia, Sept. 20–Oct. 1, 2004; p 179.

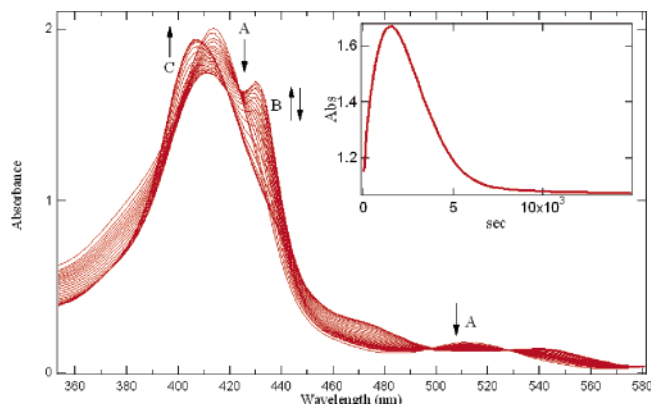


Figure 6. UV-vis absorption spectra recorded every 80.3 s after introduction of 1.6 mM NO to toluene solution containing 20 μM **1** (A, $\lambda_{\text{Soret}} = 414$ nm, $\lambda_{\text{Qband}} = 510$ nm). This is interpreted in terms of the conversion of Fe(TPP)(O₂NO) to a new species (B, $\lambda_{\text{Soret}} = 432$ nm), probably Fe(TPP)(NO₂)(NO), followed by subsequent reaction to give Fe(TPP)(NO) (C, $\lambda_{\text{Soret}} = 406$ nm). Inset: time dependence of the absorbance changes at 432 nm (B).

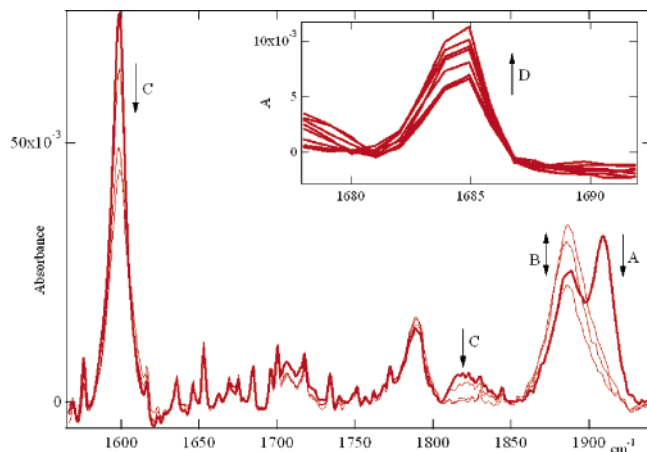


Figure 7. IR spectral changes (degassed 0.5-mm CaF₂ cell) after rapid mixing (deadtime ~ 1 s) of dichloromethane solutions containing 30 μM Fe(TPP)(NO₃) and 4.7 mM NO. The initial spectrum is taken during continuous flow through the cell, and the following spectra were accumulated approximately 1, 2, and 4 min after the flow was stopped. The quick formation and transformation of Fe(TPP)(ONO₂)(NO) (A, $\nu_{\text{NO}} = 1909$ cm⁻¹) was followed by the formation and decay of Fe(TPP)(NO₂)(NO) (B, $\nu_{\text{NO}} = 1886$ cm⁻¹). N₂O₃ was also observed to decrease (C, $\nu_{\text{NO}} = 1830$ cm⁻¹, $\nu_{\text{NO}_2} = 1600$ cm⁻¹). Inset: Eventual formation of Fe(TPP)(NO) (D, $\nu_{\text{NO}} = 1684$ cm⁻¹), initial spectrum taken 4 min after stopping the flow with the following spectra taken every 10 min.

dependencies on the rates of reaction were apparent, but it was noted that the presence of N₂O₃ stabilized **3**.

Addition of PPh₃ (as an N₂O₃ sink) to the reaction mixture, or scrupulous purification of NO prior to mixing, led to faster transformation of **3** to **1**.

A custom-made rapid flow apparatus was used in conjunction with IR measurements to help reveal the identity of the intermediates. As shown in Figure 7, rapid mixing of dichloromethane solutions of NO and Fe(TPP)(O₂NO) led to the formation of a species that displayed IR band maxima at 1909 and 1886 cm⁻¹. At longer times, the band at 1909 cm⁻¹ was found to decay, leaving the species with a band at 1886 cm⁻¹ as the dominant product. On the basis of the analogous reactions in the solid state, the band centered at 1909 cm⁻¹ was assigned as the $\nu(\text{NO})$ of Fe(TPP)(ONO₂)(NO) (**2**). Rapid mixing of dichloromethane solutions of isotopically labeled ¹⁵N¹⁸O and Fe(TPP)(O₂NO) resulted in formation of a product with a band

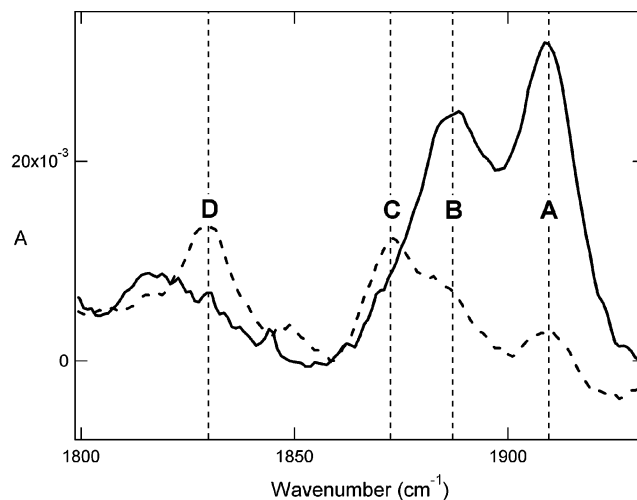


Figure 8. Infrared spectral changes (degassed 0.5-mm CaF₂ cell) during the rapid mixing (deadtime ~ 1 s) of 30 μM Fe(TPP)(NO₃) with either 4.7 mM ¹⁴N¹⁶O (dark, solid line) or 4.7 mM ¹⁵N¹⁸O (light, dashed) in dichloromethane. Reaction with ¹⁴N¹⁶O resulted in the formation of two new species with absorption peaks matching the ν_{NO} characterized for Fe(TPP)(ONO₂)(NO) (A, $\nu_{\text{NO}} = 1909$ cm⁻¹) and Fe(TPP)(NO₂)(NO) (B, $\nu_{\text{NO}} = 1885$ cm⁻¹). Reaction with ¹⁵N¹⁸O resulted in spectra that were interpreted as a mixture of Fe(TPP)(ONO₂)(¹⁴N¹⁶O) (A, $\nu_{\text{NO}} = 1909$ cm⁻¹), Fe(TPP)(NO₂)(¹⁴N¹⁶O) (B, $\nu_{\text{NO}} = 1885$ cm⁻¹), Fe(TPP)(ONO₂)(¹⁵N¹⁶O) (C, $\nu_{\text{NO}} = 1873$ cm⁻¹), and Fe(TPP)(ONO₂)(¹⁵N¹⁸O) (D, $\nu_{\text{NO}} = 1829$ cm⁻¹).

at 1829 cm⁻¹ (Figure 8). This is in agreement with the formation of Fe(TPP)(ONO₂)(¹⁵N¹⁸O) and the assignment of the isotope-sensitive absorption bands at 1909 and 1829 cm⁻¹ as the nitrosyl stretch(es) of the nitrate nitrosyl complex **2**. The other species formed under these conditions ($\nu(\text{NO}) = 1886$ cm⁻¹)¹⁴ has been characterized as Fe(TPP)(NO₂)(NO). Unfortunately, the bands expected for coordinated NO₂ or ONO (1200–1550 cm⁻¹) were obscured by solvent overtones. At longer times, the absorption bands characteristic of N₂O₃ ($\nu(\text{NO}) = 1830$ cm⁻¹, $\nu(\text{NO}_2) = 1600$ cm⁻¹)²² decreased simultaneous with the growth of a new band at 1684 cm⁻¹ characteristic of the $\nu(\text{NO})$ of Fe(TPP)(NO).

Summary

We have described here redox transformations of NO_x ligands coordinated to the heme model Fe(TPP) in the solid state as layered films and in aprotic media. The entry point to these investigations was the η^2 -nitrate complex Fe(TPP)(η^2 -O₂NO) (**1**), which undergoes a rapid NO addition step to form Fe(TPP)(η^1 -ONO₂)(NO) (**2**) (Scheme 1). In the presence of excess NO, the latter species undergoes further reaction in a process that would appear to be the result of a “simple” oxygen atom transfer from **2** to give the nitro nitrosyl complex Fe(TPP)(NO₂)(NO) (**3**). However, reactivity studies in low-temperature films using IR detection and isotope labeling techniques argue against this transformation occurring by oxygen atom transfer from the η^1 -coordinated nitrate of **2** to NO to give (initially) the nitro nitrosyl complex Fe(TPP)(ONO)(NO) (**5**) and NO₂ (scenario ii of Scheme 2). Similar arguments based on these data can be mounted against a mechanism proceeding via β -bond cleavage of the FeO–N bond of the coordinated nitrate of **2** to give a ferryl complex and NO₂ (scenario i). Neither of these scenarios can explain the isotopic distributions of products when the reactions are initiated with labeled NO or labeled **2**, unless there is significant isotopic exchange between the coordinated nitro group and the free NO.

A third pathway (scenario iii) involves Fe–O bond homolysis of **2** to give Fe(TPP)(NO) (**4**) and the $\bullet\text{NO}_3$ radical, followed by rapid trapping of this radical by excess NO to give N_2O_4 , which then reacts with **4** to give **3**. While this would indeed explain the product isotopic distributions given the demonstrated exchange between N_2O_3 and NO under these conditions, the high energy of the $\bullet\text{NO}_3$ radical would make the first step in scenario iii highly endoergic. A more palatable alternative giving the same isotopic distributions is represented above in Scheme 3. In this model, loss of the $\bullet\text{NO}_3$ radical is effected by attack of NO at the oxygen of the coordinated nitrate concerted with electron transfer to the metal center, leading to rapid dissociation of the transient N_2O_4 ligand and the formation of **4**. An analogy can be drawn between this pathway and the recently documented reductive nitrosylation of a copper(II)-coordinated amine that has been suggested to occur via such an inner sphere electron transfer process.²⁹

It is notable that the various scenarios for NO interaction with the nitrate complex **1** lead to the intermediacy of highly reactive species such as NO_2 , N_2O_3 , and N_2O_4 that contribute to oxidative and nitrosative stress and can be damaging to cellular species.³² Hence, the present study shows that under certain conditions,

the nitrate ion, usually considered relatively innocuous in mammalian systems, can be activated by NO and hemes to form other reactive NO_x intermediates.

Acknowledgment. Financial support from CRDF (Grant No. AC2-2520-TB-03), the U.S. Department of Energy (DE-FG02-04ER15506), and a Visiting Scholarship for T.S.K. at UCSB from Petroleum Research Fund is gratefully acknowledged.

Supporting Information Available: Scheme S1 showing transition of Fe(TPP)(ONO₂)(NO) to Fe(TPP)(NO₂)(NO) by mechanism of NO₃ radical elimination for mixed isotope species. Complete citations for refs 3d and 25. Figure S1 demonstrating IR spectra in the range 600–400 cm⁻¹ of thin layers containing Fe(TPP)(O₂NO) and Fe(TPP)(ONO₂)(NO), Figure S2 showing spectral changes describing formation of (NO)Fe(TPP)(O¹⁵NO₂) in the course of Fe(TPP)(O₂¹⁵NO) interaction with NO, and Figure S3 showing FTIR spectra of Fe(TPP)(ONO₂)(¹⁵NO) and Fe(TPP)(O¹⁵NO₂)(NO) isotopomers. This material is available free of charge via the Internet at <http://pubs.acs.org>.

JA042237R

(32) Kirsch, M.; Korth, H.-G.; Sustmann, R.; de Groot, H. *Biol. Chem.* **2002**, *383*, 389–399.